Water Research 190 (2021) 116748

Contents lists available at ScienceDirect

Water Research

journal homepage: www.elsevier.com/locate/watres

Electro-bioremediation of nitrate and arsenite polluted groundwater

Alba Ceballos-Escalera[a], Narcís Pous[a], Paola Chiluiza-Ramos[b], Benjamin Korth[c], Falk Harnisch[c], Lluís Bañeras[b], M. Dolors Balaguer[a], Sebastià Puig[a,*]

[a] LEQUiA, Institute of the Environment, University of Girona, C/ Maria Aurèlia Capmany, 69, E-17003, Girona, Spain
[b] Group of Environmental Microbial Ecology, Institute of Aquatic Ecology, University of Girona, C/ Maria Aurèlia Capmany, 40, E-17003, Girona, Spain
[c] Department of Environmental Microbiology, Helmholtz Centre for Environmental Research GmbH - UFZ, Permoserstraße 15, 04318 Leipzig, Germany

ARTICLE INFO

Article history:
Received 2 October 2020
Revised 7 December 2020
Accepted 12 December 2020
Available online 15 December 2020

Keywords:
Arsenic
Denitrification
Microbial electrochemical technology
Bioelectrochemical system
Continuous bioreactor
Electroactive microorganism

ABSTRACT

The coexistence of different pollutants in groundwater is a common threat. Sustainable and resilient technologies are required for their treatment. The present study aims to evaluate microbial electrochemical technologies (METs) for treating groundwater contaminated with nitrate (NO_3^-) while containing arsenic (in form of arsenite (As(III)) as a co-contaminant. The treatment was based on the combination of nitrate reduction to dinitrogen gas and arsenite oxidation to arsenate (exhibiting less toxicity, solubility, and mobility), which can be removed more easily in further post-treatment. We operated a bioelectrochemical reactor at continuous-flow mode with synthetic contaminated groundwater (33 mg $N\text{-}NO_3^-$ L^{-1} and 5 mg As(III) L^{-1}) identifying the key operational conditions. Different hydraulic retention times (HRT) were evaluated, reaching a maximum nitrate reduction rate of 519 g $N\text{-}NO_3^-$ $m^3_{\text{Net Cathodic Compartment}}$ d^{-1} at HRT of 2.3 h with a cathodic coulombic efficiency of around 100 %. Simultaneously, arsenic oxidation was complete at all HRT tested down to 1.6 h reaching an oxidation rate of up to 90 g As(III) $m^{-3}_{\text{Net Reactor Volume}}$ d^{-1}. Electrochemical and microbiological characterization of single granules suggested that arsenite at 5 mg L^{-1} did not have an inhibitory effect on a denitrifying biocathode mainly represented by *Sideroxydans* sp. Although the coexistence of abiotic and biotic arsenic oxidation pathways was shown to be likely, microbial arsenite oxidation linked to denitrification by *Achromobacter sp.* was the most probable pathway. This research paves the ground towards a real application for treating groundwater with widespread pollutants.

1. Introduction

Groundwater constitutes the largest reservoir of drinking water. However, the presence of different pollutants compromises its usage (European Commission, 2008). The coexistence of several and different types of contaminants from anthropogenic and geological sources is a common thread that requires the development of sustainable technologies capable of treating these mixtures of pollutants (Zhang et al., 2017). The World Health Organization (WHO) has defined nitrate and arsenic as hazardous inorganic contaminants in groundwater (WHO, 2017). Nitrate is one of the most widespread pollutants in groundwater due to intensive agriculture and has become a worldwide concern. For human health and safety, the Nitrates Directive (91/767/EU) sets a nitrate concentration limit of 11.3 mg $N\text{-}NO_3^-$ L^{-1} in drinking water. Conventional nitrate-polluted groundwater treatments are usually based on separation technologies. Besides being effective, these technologies are energy-intensive (1.03-2.56 kWh m^{-3}_{treated}) and produce waste brines demanding additional post-treatment (Twomey et al., 2010). Other conventional treatments are based on biological denitrification by a sequential reduction of nitrate to dinitrogen gas (N_2) through four reduction steps (Table 1). Although biological treatments hold environmental and economic advantages, electron donors are limited in groundwater and a continuous supply of chemicals such as acetate or hydrogen gas is required.

Electro-bioremediation is a primary microbial electrochemical technology (MET) and emerges as a sustainable alternative for groundwater treatment (Pous et al., 2018). MET is based on bioelectrochemical systems (BES) harnessing the capacity of electroactive microorganisms to perform oxidation and reduction reactions with solid electron conductors (e.g., electrodes). Thereby, these electroactive microorganisms are able to use the anode and

* Corresponding author at: LEQUiA, Institute of the Environment, University of Girona, C/ Maria Aurèlia Capmany, 69, E-17003, Girona, Spain.
E-mail address: sebastia.puig@udg.edu (S. Puig).

https://doi.org/10.1016/j.watres.2020.116748

Table 1
Standard Redox potentials at biological standard conditions (25°C, pH 7).

Reaction	$E^{o'}$ (V *vs.* SHE)
Nitrate / Dinitrogen gas	
$NO_3^- + 2H^+ + 2e^- \rightleftarrows NO_2^- + H_2O$	+0.43
$NO_2^- + 2H^+ + 1e^- \rightleftarrows NO + H_2O$	+0.36
$NO + H^+ + 1e^- \rightleftarrows \frac{1}{2}N_2O + \frac{1}{2}H_2O$	+1.18
$N_2O + 2H^+ + 2e^- \rightleftarrows N_2 + H_2O$	+1.36
Arsenite / Arsenate	
$H_3AsO_4 + 2H^+ + 2e^- \rightleftarrows H_3AsO_3 + H_2O$	+0.02

the cathode as an inexhaustible electron acceptor or donor, respectively (Logan et al., 2019). When nitrate is the target pollutant, autotrophic denitrification can be performed using only the cathode as electron donor and inorganic carbon as carbon source (Clauwaert et al., 2007). So far, denitrification by MET have been widely studied ranging from a first proof of concept (Gregory et al., 2004) to investigations on the underlying mechanism to technological applications (Clauwaert et al., 2009; Virdis et al., 2008). Few studies showed nitrate treatment in combination with other contaminants performed by MET to identify potential electron donor/acceptor competitors or inhibitory effects. The literature has been mostly focused on organic compounds and sulfate (Lai et al., 2015; Nguyen et al., 2016a).

Arsenic contamination of groundwater in many cases occurs naturally due to reductive dissolution of arsenic-rich minerals. The World Health Organization (WHO) has established a temporal guideline value of 10 μg L^{-1} as a permissive limit for drinking water (WHO, 2017). The predominant oxidation states of inorganic arsenic are arsenite (As(III)) and arsenate (As(V)). In reducing conditions, arsenic is mostly found as arsenite, which is the most toxic, soluble, and mobile form. In line with this, the groundwater redox potential has an essential role in the arsenic-contaminated groundwater. In general, it has been observed that the reductive arsenic dissolution can be low in nitrate-contaminated groundwater (Hosono et al., 2011). However, arsenic and nitrate do co-exist in groundwaters that present a high content of bicarbonate (Piqué et al., 2010), due to punctual arsenic dissolution related to drought periods (Ventura-Houle et al., 2018), or punctual industrial dumpings/leakages (e.g., some industrial activities that include the use of insecticides, pesticides and wood preservatives) (Jang et al., 2016).

Arsenic removal in water treatment is traditionally carried out by arsenite oxidation to arsenate (Table 1) as a preliminary step to decrease the arsenic solubility followed by precipitation using metal salts (Borho and Wilderer, 1996). Adsorption-based removal methods (i.e. granulated ferric hydroxide) are more effective also with arsenate (Banerjee et al., 2008). Arsenite oxidation to arsenate is conventionally performed by chemical oxidation by ozone, iron and manganese oxide, or photochemical oxidation (Bissen and Frimmel, 2003) (standard redox potential shown in Table 1). However, these oxidation methods have low selectivity resulting in toxic by-products generation such as nitroaromatic compounds (Ji et al., 2017). Besides, chemical treatments are characterized by constant chemical consumption and the possible use of catalysts, resulting in a high operational cost (Wang and Zhao, 2009). Recently, an environmentally-friendly process for arsenite oxidation using microorganisms as sustainable catalysts is attracting interest. In environments lacking organic matter, e.g., groundwater, autotrophic bacteria can be applied to oxidise arsenite using external oxygen or nitrate as electron acceptor (Crognale et al., 2017; Wang et al., 2017). For instance, arsenite can be linked to denitrification by some microorganisms. Nevertheless, arsenite can inhibit chemolithotrophic denitrification in a wide range of concentrations. In adapted microbial communities, inhibition was found

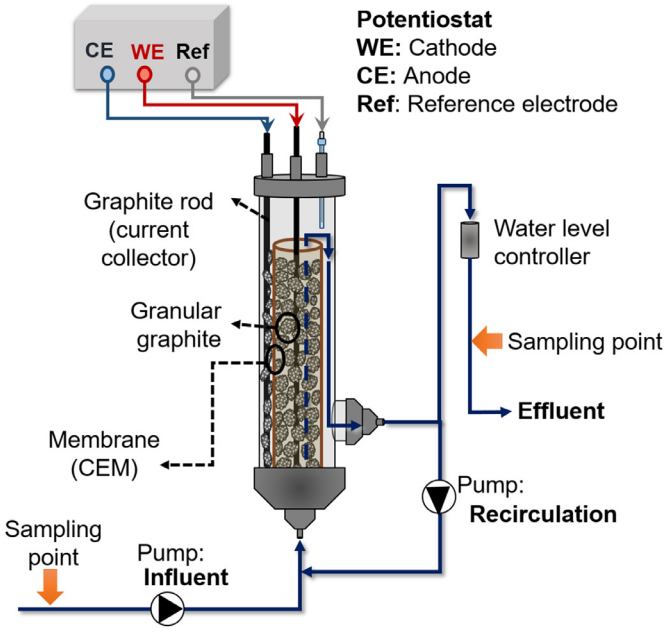

Fig. 1. Scheme of the reactor used in experimental study – details see text.

in the range of 150 to 375 mg As(III) L^{-1} (Sun et al., 2009, 2008). Recent studies indicated that METs represent a novel and suitable approach to arsenite oxidation to arsenate (Li et al., 2016; Nguyen et al., 2016b, 2017; Pous et al., 2015a).

The present study proposes a bioelectrochemical system to treat nitrate-contaminated groundwater that contains arsenic as a co-contaminant. Arsenic was included in form of arsenite over arsenate due to its higher toxicity and mobility. The main goal is the exploration whether nitrate can be successfully converted into dinitrogen gas having arsenic in the same water while pursuing arsenite oxidation at the same time. So far, one preliminary study demonstrated the combined electrochemical treatment of arsenic and nitrate in a single reactor. Nguyen et al. (2016b) coupled anodic arsenite oxidation and cathodic denitrification in a compartmentalized system, where enriched arsenic and nitrate solutions were separately fed to the anodic and cathodic compartment, respectively. The present study explores the presence of both pollutants in the same water matrix. A novel continuous-flow MET was developed and operated for simultaneous nitrate removal and arsenite oxidation. Thereby, the operational conditions (e.g., recirculation and hydraulic retention time) were adapted for treating groundwater. Furthermore, the effects of arsenite on denitrifying biocathode performance were investigated and arsenite oxidation pathways were elucidated.

2. Materials and methods

2.1. Reactor setup

Two identical tubular BES reactors were assembled and operated as replicates (reactor A and B). Fig. 1 schematically presents the reactor configuration used in this study. The anode and cathode were separated by a tubular cation exchange membrane with an internal diameter of 45 mm (CEM, CMI-7000, Membranes Int., USA). The structure was built with PVC tube (diameter of 55 mm and length of 350 mm). The cathode (inner part) and anode (outer part) compartments were filled with granular graphite (diameter 1.5-5 mm, enViro-cell, Germany; previously washed with 1 M HCl and 1 M NaOH) and graphite rods (8 × 400 mm and 4 × 2500 mm for cathode and anode compartment, respectively; Mersen Ibérica,

Spain) were used as current collectors. Assuming that each chamber was filled with spherical particles (average diameter of 3.25 mm) with a fixed bed porosity of 50 %, electrode surfaces of 0.51 m^2 and 0.29 m^2 were calculated for the cathode and anode compartment, respectively. The net liquid volumes of cathode (NCC) and anode (NAC) compartment were 0.3 L and 0.15 L, respectively. The reactors were equipped with an Ag/AgCl sat. KCl reference electrode (+0.197 V vs. standard hydrogen electrode, SHE, SE 11, Xylem Analytics Germany Sales GmbH & Co. KG Sensortechnik Meinsberg, Germany) resulting in a three-electrode setup. The cathode potential was poised at -0.123 V *vs*. SHE using a potentiostat (VSP, BioLogic, France) to drive complete nitrate reduction to dinitrogen gas according with previous knowledge (Pous et al., 2015b). If not stated otherwise, all redox potentials are provided in respect of SHE.

The cathode and the anode were hydraulically connected. The influent was directly pumped upwards through the cathode compartment and spilled over at its top to the anode compartment. Subsequently, it circulated from the top to the bottom of the anode compartment, where the outlet was located. In certain operational periods, a fraction of the effluent was recirculated to the influent to increase internal flow (Fig. 1). The recirculation increased the fluid velocity in the cathode compartment from 1×10^{-5} m s^{-1} (without recirculation) to 4×10^{-4}, and 9×10^{-4} m s^{-1}, with recirculation flow rate of 35 L d^{-1} and 85 L d^{-1}, respectively. The increase of the internal fluid velocity reinforced the mass transfer of substrate as well as counter ions from the bulk liquid to inner biofilm layers. Additional benefits were the decrease of possible dead zones and increase homogeneity inside the reactor.

2.2. Reactor inoculation

The anode and cathode compartments were simultaneously inoculated for 30 days before the continuous operation. A solution was prepared containing 79 % of synthetic groundwater, 20 % of effluent from a denitrifying BES reactor (Pous et al., 2017) and 1 % of an enriched autotrophic arsenite oxidizing culture. This solution was used to fill both reactors and an external 1 L tank. The influent and the effluent of the reactors were connected to the 1 L tank and a peristaltic pump was used to continuously recirculate the solution at a flow rate of 35 L d^{-1} (i.e., closed-loop mode). When nitrate and arsenite were depleted (i.e., concentrations of both compounds were below 1 mg L^{-1}), the medium of the 1 L tank was replaced with a fresh solution. The cathode potential was poised at -0.123 V to promote growth of denitrifying bacteria.

Autotrophic arsenite-oxidizing culture was obtained from arsenic contaminated sites in the province of Girona (Spain). Samples were collected from surface and contaminated groundwater (seven samples). Each sample (25 mL) was added to 125 mL of mineral medium without any organic carbon source with a final concentration of 15 mg As(III) L^{-1} following the same methodology as described in Pous et al. (2015a). Each sample was incubated aerobically by constant aeration at room temperature (20 ± 2°C) and with constant agitation (200 rpm). After 50 days, the enriched microorganisms were sub-cultured in a fresh mineral medium in a dilution of 1 %. All sub-cultured enrichments showed a mean arsenite oxidation rate of 0.4 ± 0.2 g As(III) m^{-3} d^{-1} without any observable differentiation between the enrichments. These sub-cultured enrichments were blended, resulting in the enriched autotrophic arsenite oxidizing culture used for inoculation of reactors A and B.

2.3. Reactor continuous operation

After the inoculation period, the reactors were operated in continuous flow mode at 1.4 L d^{-1} (hydraulic retention time, HRT, of 7.5 h) without recirculation flow using synthetic groundwater. After 25 days, the reactors were operated applying a recirculation flow of 35 L d^{-1} to reinforce the substrate distribution and promote mass transfer. Following these operating conditions, the HRT was progressively decreased from 7.5 to 1.6 h. Two recirculation flow rates were tested: (i) from HRT of 7.5 to 4.4 h with a recirculation flow rate of 35 L d^{-1} and (ii) from HRT of 5.0 to 1.6 h with a recirculation flow rate of 85 L d^{-1}. An overview of all tests is listed in Table S1 (Supplementary data). Each condition had a minimum duration of 7 days.

2.4. Synthetic groundwater

Synthetic medium mimicking nitrate and arsenic contaminated groundwater was used to feed the reactors. The synthetic groundwater was prepared considering the main characteristics of groundwater from Navata village, Girona (Spain) (28 ± 6 mg N-NO_3^- L^{-1}, 1.0 ± 0.1 mS cm^{-1} and pH of 8.0 ± 0.2, Pous et al., 2013). The arsenic in groundwater is typically in the concentration range of some µg L^{-1} (Van Halem et al., 2009). At the sample site of Navata (Spain), the arsenic concentration was below 10 µg L^{-1}. Nevertheless, the arsenite concentration was adjusted to high concentration of 5 mg As(III) L^{-1} to test the potential of the system under more severe conditions.

The synthetic groundwater was prepared with distillate water and contained 203.9 mg L^{-1} $NaNO_3$ (33 mg N-NO_3^- L^{-1}), 8.7 mg L^{-1} $AsNaO_2$ (5 mg As(III) L^{-1}), 420.0 mg L^{-1} $NaHCO_3$ as inorganic carbon source, 7.5 mg L^{-1} KH_2PO_4, 1.9 mg L^{-1} Na_2HPO_4, 100.0 mg L^{-1} NaCl, 75.2 mg L^{-1} $MgSO_4 \times 7H_2O$, 10.0 mg L^{-1} NH_4Cl and 0.1 mL L^{-1} of a trace minerals solution (Balch et al., 1979). In addition, the influent contained 10% of effluent from a denitrifying BES reactor (Pous et al., 2017) during all operational periods to simulate the presence of microorganisms in the groundwater. This effluent with a OD_{600} of 0.05 was composed by *Proteobacteria* phylum (78%) being *Acidithiobacillus* sp. as the most abundant genus. The electric conductivity of the synthetic groundwater was 1.3 ± 0.2 mS cm^{-1} and the initial pH was 8.1 ± 0.2 for simulating groundwater from Navata, Girona (Spain).

2.5. Abiotic arsenite oxidation tests

A series of abiotic tests were performed to determine chemical (using nitrate and oxygen) and electrochemical arsenite oxidation. In addition, the putative role of granular graphite as catalyst for arsenite oxidation and its arsenic sorption capacity were also investigated. All abiotic tests are shown in Table 2 and experiment setups are shown in Supplementary data, Figure S1. Each test was performed in duplicates for 24 h in batch mode using 100 mL flasks with 75 mL of synthetic groundwater (as described above).

Anoxic (with nitrate) and aerobic tests were performed in the absence and presence of granular graphite. In addition, an aerobic test was also performed in presence of PVC granules as non-conductive material. The corresponding tests used 50 mL of granular graphite or of PVC granules; both materials with an average diameter of 3.5 mm and estimated surface of 0.05 m^2. Anoxic conditions were established by flushing the medium with N_2 during 10 minutes before each test. The tests under aerobic conditions were carried out under continuous aeration using a domestic aquarium air pump. Finally, the electrochemical arsenite oxidation was studied with a granular graphite bed poised at +1.15 V by a potentiostat (NAV 3.2, NANOELECTRA, Spain). In the electrochemical test, a single-chamber configuration was used with a three-electrode setup using two graphite rods (diameter 6 mm, Mersen Ibéria, Spain) serving as current collector for the granular graphite bed (working electrode) and as counter electrode, and a Ag/AgCl sat. KCl electrode as reference electrode

Table 2
Experimental conditions and results of abiotic tests for arsenite oxidation within 24 h. Results represent mean values with standard deviations (n>2).

Electron acceptor	Presence of granular graphite	Efficiency of arsenite oxidation (%)	Maximum arsenite oxidation rate (mgAs(III) $m_{anode}^{-2}d^{-1}$)
Nitrate	No	Not detected	Not detected
Nitrate	Yes	Not detected	Not detected
Nitrate	No	Not detected	Not detected
Oxygen	*No	5±2	-
Oxygen	Yes	45±7	3.4±0.2
Anode potential at +1.15 V	Yes	75±5	6.5±0.1

*With presence of PVC granules as a non-conductive material.

2.6. Electrochemical characterization of isolated granules

The granular graphite from both BES reactors was further characterized using electrochemical measurements. The present study uses an improved version of the e-Clamp firstly introduced by (Rodrigo Quejigo et al., 2018). The improved e-Clamp consists of four spring steel wires (1.4310, Febrotec GmbH, Germany) forming a gripper that is encased by a PEEK tube (Figure S2, Supplementary data). The e-Clamp can be mechanically moved. The electrochemical experiments were conducted in a four-neck round-bottom flask (Lenz Laborglas GmbH & CO.KG, Germany) with an integrated three-electrode setup with a graphite rod as counter electrode (10 × 50 mm, Mersen Ibéria, Spain) and with an Ag/AgCl sat. KCl as reference electrode. Thereby, the working electrode was the e-Clamp holding three granules per test with an average wet weight of 0.31 ± 0.01 g (directly measured after each test). The sampled granules for electrochemical measurements were taken in triplicates during operation at HRT of 1.6 ± 0.1 h (days 187-194) from: (i) the top of the cathode compartment of both reactors and (ii) the bottom of the anode compartment of reactor B. Abiotic controls were performed using non-inoculated granular graphite. The experiments were carried out at room temperature (23 ± 2°C), with constant agitation (magnetic stirring, 150 rpm) and with continuous flushing of N_2 to ensure anoxic conditions.

Directly after sampling, granules were immersed in synthetic groundwater medium without nitrate nor arsenite (buffer / non-turnover conditions) and chronoamperometry (CA) was performed with the working electrode poised at -0.12 or +0.50 V for the cathodic and anodic (Pous et al., 2015a) granules, respectively. When current density reached a stable value, cyclic voltammetry (CV) was conducted in a potential range from -0.60 to +0.20 and +0.20 to +1.00 V for the cathodic and anodic granules, respectively. Three cycles were performed at scan rate of 1 mV s^{-1}, the third cycle was used for data analysis by SOAS (Fourmond et al., 2009). After CV, the CA was switched to turnover conditions. Thereby, cathodic granules were tested by sequential addition of nitrate (33 mg N-NO_3^- L^{-1}) and arsenite (5 mg As(III) L^{-1}) to the same medium. Anodic granules were tested under turnover conditions by addition of arsenite to the medium (5 mg As(III) L^{-1}).

2.7. Analytical methods and calculations

Samples of effluent and influent were taken and analysed from both reactors three times per week, resulting in a minimum of three analytical measurements for each condition. All liquid samples were analysed according to APHA standard water measurements (APHA, 2005) for nitrate (N-NO_3^-), nitrite (N-NO_2^-), and arsenate (As(V)) by ionic chromatography (ICS 5000, Dionex, USA). Total arsenic was analysed by adding an oxidizing agent (100 mM $KMnO_4$) to fully oxidize all arsenic forms into arsenate. Arsenite concentration was calculated as the difference between total arsenic and arsenate. Three measurements of arsenic forms to the arsenic balance were obtained: Total arsenic, arsenite and arsenate. The pH and electrical conductivity of the samples were measured with a pH-meter (pH-meter basic 20^+, Crison, Spain) and a conductivity meter (EC-meter basic 30^+, Crison, Spain), respectively. Nitrous oxide (N_2O) was measured once per week using a N_2O liquid-phase microsensor (Unisense, Denmark) located in the effluent of the reactors.

The hydraulic retention time was calculated considering the net cathodic volume (HRT_{cat}) and whole net reactor volume (HRT) for denitrification and arsenite oxidation, respectively. In order to analyse the performance of each condition in continuous operation, nitrate reduction (rNO_3^-) and arsenite oxidation (rAs(III)) rates were calculated (Eq. S1 and S4, Supplementary data). The coulombic efficiency of denitrifying biocathode (CE_{cat}) was calculated as proposed Pous et al. (2017). It was calculated considering all reduction steps from nitrate to dinitrogen gas considering nitrite and nitrous oxide accumulation (Eq. S6, Supplementary data). For the arsenite oxidation at the bioanode, anodic columbic efficiency (CE_{an}) were calculated considering the oxidation from arsenite to arsenate (Eq. S8, Supplementary data).

2.8. Microbiological analysis

Granular graphite was sampled for DNA extraction two times from the upper part of the anode and cathode compartment of running reactors at HRT of 2.8 and 2.3 h (day 145 and 180). DNA was extracted as described previously in Vilajeliu-Pons et al. (2016). The obtained DNA was quantified using a NanoDrop ND-1000 spectrophotometer (NanoDrop Technologies Inc., Wilmington, USA) and stored at -20°C. Illumina MiSeq flow cell (V2) sequencing was conducted by the RTSF Core facilities at the Michigan State University USA (https://rtsf.atsci.msu.edu/). The primers 515F and 806R were used for the amplification of the V4 region of 16S rDNA according to the method described by Kozich et al. (2013).

Sequence data from the MiSeq platform were quality filtered, trimmed, dereplicated, merged, and, after a process of chimera removal, were clustered into amplicon sequence variants (ASVs) using the DADA2 Pipeline (Callahan et al., 2016). Afterwards, ASVs tabulation and taxonomy assignment were performed using the Silva taxonomic database (v132). Finally, the Phyloseq package was used to tabulate relative abundances at various taxonomic levels (McMurdie and Holmes, 2013). All analyses were performed with R (v.3.6.3) using packages dada2 v.1.14.1 and phyloseq v. 1.30.0. Representative sequences for each amplicon sequence variant ASVs were assigned taxonomically using Blast searches at NCBI.

3. Results and discussion

3.1. Denitrification and arsenite oxidation performance in METs

Both reactors were operated as replicates in continuous flow mode after the inoculation period. The cathode potential was controlled at -0.123 V to promote denitrifying biocathodes (Pous et al., 2015b) while arsenite oxidation was expected to occur in the anode compartment. Fig. 2A and B show the nitrate and arsenite

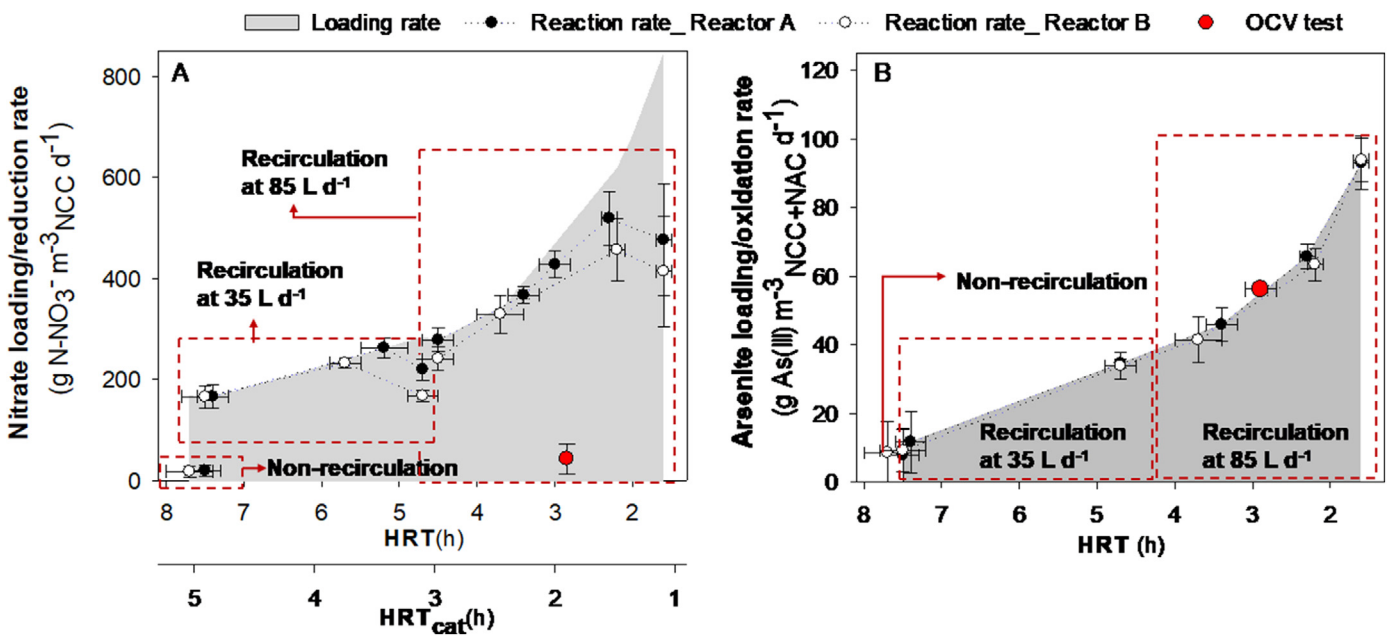

Fig. 2. A) Nitrate loading and reduction rates and B) arsenite loading and oxidation rates of reactor A and B at different hydraulic retention times (HRTs) and recirculation flows. It also shows an experiment with reactor A being operated under open circuit voltage condition (OCV). Results represent mean values and error bars represent standard deviations of analytical replicates during each operational condition (n≥3).

loading and reduction rates. The continuous operation started with HRT of 7.5 ± 0.3 h (HRT_{cat} of 5.0 ± 0.3 h) without recirculation. After 13 days, the reactor reached a steady-state performance with a nitrate reduction rate (rNO_3^-) of 24 ± 10 g $N\text{-}NO_3^-$ m^{-3}_{NCC} d^{-1} (nitrate removal of 15 ± 5 %). Although nitrate was removed at a low rate, it was completely reduced to dinitrogen gas with low nitrite accumulation (3.4 ± 3.0 % of nitrogen removed) and no nitrous oxide emissions were detected (Table S1, Supplementary data). Hence, about >95 % of the nitrate was reduced into dinitrogen gas.

The low denitrification rate compared to previous studies (849 g $N\text{-}NO_3^-$ m_{NCC}^{-3} d^{-1}, Pous et al., 2017) could be mainly explained by mass transfer limitations. The low fluid velocity in the cathode compartment during the operation (1×10^{-5} m s^{-1}) resulted in a limited mass transfer restricting catalytic rates. Moreover, the low mass transfer also affects the transfer of charge balancing ions (mainly sodium but also protons) outwards the electroactive biofilm, inhibiting electrochemical reactions (Puig et al., 2012). To reduce limitations and to enhance denitrification performance, the fluid dynamics of the reactors was improved by including a recirculation. A recirculation flow of 35 L d^{-1} (25-fold more compared to the influent) at the same HRT_{cat} of 5 h resulted in an improved rNO_3^- of 166 ± 22 g $N\text{-}NO_3^-$ m^{-3}_{NCC} d^{-1} representing a 7-fold increase compared to previous operation without recirculation. Thereby, nitrate removal increased to 99 ± 1 % in both reactors without accumulation of neither nitrite nor nitrous oxide. Recirculation reduced the pH in the cathode compartment from 9.0 ± 0.2 to 8.0 ± 0.3 due to an improved transport of protons between both compartments. Thus, the denitrifying performance was enhanced as the pH was closer to the optimal pH of 7 (Clauwaert et al., 2009; Glass and Silverstein, 1998; Wang et al., 2018). Subsequently, HRT_{cat} was continuously decreased to increase the nitrate loading rate while maintaining the recirculation flow at 35 L d^{-1} (Fig. 2A). The nitrate reduction rate increased in both reactors until the HRT_{cat} was reduced to 3.6 ± 0.2 h resulting in a nitrate reduction rate of 247 ± 22 g $N\text{-}NO_3^-$ m^{-3}_{NCC} d^{-1} (99±1 % nitrate removal). However, the nitrate removal decreased to 54 ± 10 % at a lower HRT_{cat} of 3.0 ± 0.2 h.

Therefore, the recirculation was increased from 35 to 85 L d^{-1} to overcome the above mentioned denitrification limitations. As result at HRT_{cat} of 3.0 ± 0.2 h, the denitrification performance was recovered in both reactors reaching nitrate removal of 91 ±10 %. The HRT_{cat} was further decreased to 1.5 ± 0.1 h to explore the maximum nitrate removal rate resulting in rNO_3^- of 519 ± 53 g $N\text{-}NO_3^-$ m^{-3}_{NCC} d^{-1} (90 ± 6 % of nitrate removed) and 456 ± 61 g $N\text{-}NO_3^-$ m^{-3}_{NCC} d^{-1} (71 ± 13 % of nitrate removed) of reactors A and B, respectively. At this condition, the effluent from both reactors achieved the quality standards for drinking water regarding nitrate and nitrite concentration (<11 mg $N\text{-}NO_3^-$ L^{-1} and <0.15 mg $N\text{-}NO_2^-$ L^{-1}, Table S1 in Supplementary data) according to Nitrates Directive, 91/767/EU. Moreover, no nitrite accumulation was observed and the emitted nitrous oxide only represented 3.5 ± 2.0 % of removed nitrate. In consequence, it can be considered that about >95 % of removed nitrate was converted into dinitrogen gas. Besides working at relatively high pH (around 8.0 at both influent and effluent) could imply the accumulation of denitrification intermediates (Glass and Silverstein, 1998; Molognoni et al., 2017), such accumulation was not detected in our study. Further decreasing HRT_{cat} to 1.1 ± 0.1 h resulted in lower nitrate reduction rates of 444 ± 90 g $N\text{-}NO_3^-$ m^{-3}_{NCC} d^{-1} in both reactors. Thereby, the nitrate removal decreased to 51 ± 11 %.

Arsenite oxidation to arsenate was stable in both reactors during the whole experimental period, reaching arsenite concentrations below the analytical quantification limit (0.1 mg As(III) L^{-1}). The maximum arsenite oxidation rate (rAs(III)) was 92 ± 5 g As(III) $m^{-3}_{NAC+NCC}$ d^{-1} at HRT of 1.6 ± 0.1 h, well above the maximum reported volumetric arsenite oxidation rate in METs (30 g As(III) m^{-3} d^{-1}, Nguyen et al., 2016b). However, considerably higher biological arsenite oxidation rates are reported using nitrate as the electron acceptor, e.g., 1000 mg As(III) L^{-1} d^{-1} in continuous granular sludge reactors (Sun et al., 2009). Nevertheless, the observed trend of rAs(III) during the tested HRTs (Fig. 2B) suggests that the maximum oxidation rate was not reached under the applied exper-

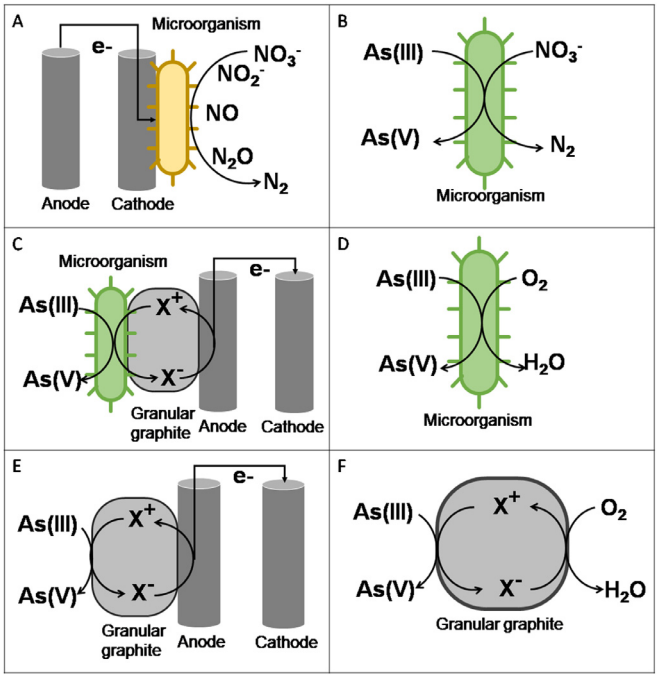

Fig. 3. Schematic illustration of possible abiotic and biotic coexistence pathways in the reactors. (A) Bioelectrochemical nitrate reduction, (B) biological arsenite oxidation linked to denitrification, (C) bioelectrochemical arsenite oxidation, (D) biological arsenite oxidation using oxygen as electron acceptor, (E) electrochemical arsenite oxidation through granular graphite, (F) chemical arsenite oxidation using oxygen as electron acceptor catalyzed by granular graphite. (X: redox-active compounds).

imental conditions and lower HRT would probably lead to higher rAs(III). The effluent pH was at the upper limit for biological arsenite oxidation according to previous studies (optimum pH between 6 and 8) (Bachate et al., 2012). Arsenic concentrations were stable at 6.4 ± 1.1 mg L^{-1} in the influent/effluent. No decrease of total arsenic was observed during the 194 days of reactor operation, suggesting negligible arsenic adsorption / precipitation inside the BES reactor.

The CE_{cat} based on the electron balance for reduction of nitrate to dinitrogen gas reached values close to 100 % in both reactors (Table S1, Supplementary data). It suggested that secondary reactions (e.g. oxygen reduction or arsenate reduction) were not significantly occurring at the cathode. Arsenic stabilized in form of arsenate (less mobile easy to adsorb form) over the reactor operation, in spite of the reductive environment of the cathode. In the range of the measured anode potentials (+0.56 ± 0.13 to +1.87 ± 0.33 V, Supplementary data, Figure S3), biological arsenite oxidation has been reported (Pous et al., 2015a). However, if it is considered that arsenite oxidation to arsenate was the main anode reaction, a CE_{an} of 2.0 ± 0.7 % is obtained. Thus, secondary reactions such as graphite (Lai et al., 2017) and water oxidation were required to provide the electrons for the denitrifying biocathode. The arsenite oxidation pathways in the reactors were further investigated in the following section.

3.2. Arsenite oxidation pathways

Due to the coexistence of different terminal electrons acceptors in these BES reactors, arsenite oxidation could proceed via different pathways (Fig. 3 B-F): (i) the anode; (ii) nitrate; and (iii) oxygen formed by water oxidation at the anode. For this reason, abiotic and biotic tests were performed with the three possible acceptors in the absence and presence of graphite granules to elucidate the predominant pathways.

Table 2 summarizes the results of abiotic 24 h tests in batch-mode. Oxygen has been reported as an oxidant capable of arsenite oxidation at a low rate (Bissen and Frimmel, 2003). No oxidation was detected under constant aeration without granular graphite during 24 h due to low oxygen dissolution from the air bubbles to the liquid phase. When a PVC granules bed was added to the setup, littler air bubbles could be formed, improving oxygen diffusion. This slightly increased the maximum arsenite oxidation rate to 0.2 ± 0.1 mg As(III) L^{-1} d^{-1} (oxidation of 5 ± 2 %). However, maximum arsenite oxidation rate was improved by 10-fold in presence of granular graphite under aerobic condition (rAs(III) of 2.1 ± 0.5 g m^{-3} d^{-1}, 45 ± 7 %). In addition, polarizing granular graphite at +1.15 V (potential in the range of anode potentials during reactors operation) yielded an even higher oxidation rate (4.0 ± 0.1 g m^{-3} d^{-1}, 75 ± 5%). At this condition, arsenite could be directly oxidized by the anode ($E^{o'}$ = 0.02 V at pH 7, Table 1) or via oxygen that can be formed by water oxidation ($E^{o'}$ = +0.81 V at pH 7). The considerably improved arsenite oxidation rate in the presence of granular graphite compared to a non-conductive material (PVC) suggested a catalytic role of granular graphite. Furthermore, no variation of total arsenic (<1%) was measured during the abiotic tests. This supports the results observed in the bioreactors (Section 3.1), suggesting that arsenic adsorption/precipitation was negligible.

To our knowledge, it is not reported in literature that pure carbon materials (e.g., pure graphite) have catalytic properties for the arsenite oxidation. However, granular graphite from its production process can contain some impurities that could possess a catalytic role. Elemental analysis of granular graphite revealed the presence of iron at a concentration of 5.7 ± 0.2 mg Fe $Kg_{graphite}^{-1}$ (Table S2, Supplementary data). For example, some studies report that carbon materials supplemented with iron can oxidize and absorb arsenite (Chen et al., 2007). Furthermore, electrochemical analysis of abiotic granular graphite with the e-Clamp (Fig. 4A and C) showed an oxidative peak at +0.55 V in CVs in the absence and in the presence of arsenite (non-turnover and turnover condition, respectively). This further indicates that redox-active compounds were present in granular graphite (e.g., iron or quinones). Further, the current density increased in abiotic CV at turnover condition at a voltage between of +0.55 to +1.00 V compared to CV at non-turnover condition (Fig. 4A and C), suggesting the electrochemical arsenite oxidation using granular graphite (Fig. 3E).

The arsenite oxidation rate observed in the electrochemical abiotic test using the anode as electron acceptor (6.5 ± 0.1 mgAs(III) m_{anode}^{-2} d^{-1}) and the abiotic test in the presence of oxygen (3.4 ± 0.2 mg As(III) m_{anode}^{-2} d^{-1}) can only explain the observed arsenite oxidation rate in the BES (142 ± 7.7 mgAs(III) m_{anode}^{-2} d^{-1} at lower HRT of 1.6h) to a minor extent (<10%). The role of biological arsenite oxidation independent of electrochemical pathways was analysed by operating reactor A under open circuit voltage (OCV) conditions at HRT of 2.9 ± 0.1 h. Under these conditions, complete arsenite oxidation was observed (>95 %) with a rAs(III) of 91.5 ± 1.5 mgAs(III) m_{anode}^{-2} d^{-1} (59 ± 1 g As(III) $m^{-3}_{NAC+NCC}$ d^{-1}, Fig. 2B). This suggested the capacity of the microbial community to oxidize arsenite without current supply. During OCV, the denitrification rate was 43 ± 12 g $N\text{-}NO_3^-$ m^{-3}_{NCC} d^{-1} (7 ± 2 % of nitrate removed) and the conversion was virtually complete to N_2 (Table S1, Supplementary data). In this period, the observed molar ratio between arsenite oxidation and nitrate reduction was 0.4 ± 0.1 (As:N). This is in a good concordance with the theoretical molar ratio of 0.4 (As:N) considering the electrons provided by As(III) oxidation to As(V) and the electrons required for NO_3^- reduction to N_2. Therefore, the possibility of arsenite oxidation linked to denitrification in the reactor is proved (Fig. 3B) and is substantially

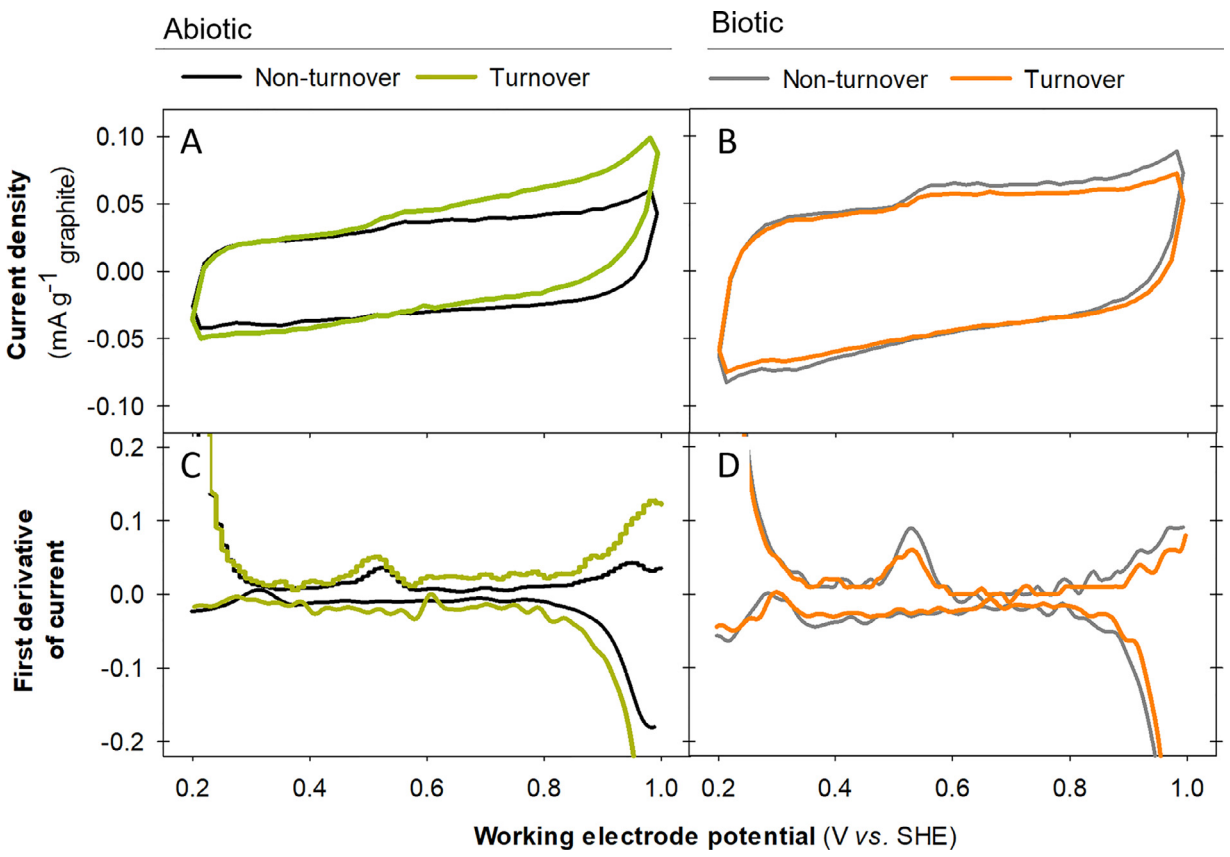

Fig. 4. Turnover and non-turnover CVs of granular graphite performed with e-Clamp at scan rate of 1 mV s-1 and corresponding first derivatives of non-inoculated granular graphite (A and C, respectively) and inoculated granular graphite extracted from the anodic compartment of reactor B (B and D, respectively). Only 3rd scans are shown.

contributing to the overall arsenite oxidation. However, it cannot be fully excluded that also aerobic arsenite oxidation (Fig. 3D) occurred in the reactors due to accumulation of oxygen formed by water oxidation prior to OCV or by air intrusions. Additional electrochemical analysis of granular graphite sampled from the anodic compartment of reactor B was performed to reveal if bioelectrochemical arsenite oxidation also played a role in the inoculated reactor. However, there are no remarkable differences between turnover and non-turnover CVs of inoculated graphite granules indicating that bioelectrochemical arsenite oxidation is of minor importance under the tested experimental conditions (Fig. 4B and D).

Taking all results together, the both abiotic and biotic arsenite oxidation pathways in the studied METs was demonstrated. Thereby, arsenite oxidation was mainly performed by microorganisms using nitrate electron acceptors (Fig. 3B), associating the denitrification with arsenite oxidation. Nevertheless, electrochemical oxidation (Fig. 3E) and abiotic oxidation with oxygen catalysed by granular graphite (Fig. 3F) was also demonstrated with a minor influence on total arsenite oxidation.

3.3. Microbial community

The microbiological communities of the reactors A and B were analysed through DNA extraction of granular graphite of both compartments at HRT of 2.8 and 2.3 h (day 145 and 180). The analysis was performed at genus level of most abundant ASVs by BLASTn searches (Table 3).

The biocathode inhabited a complex microbial community predominantly composed of *Proteobacteria* (81-89% in reactor A and B, respectively). *Betaproteobacteriales* accounted for up to 68-84% of all sequences. The taxon is characterized to contain bacterial species with a broad range of metabolic capabilities, including redox transformation of metals (e.g., iron and arsenic) and denitrification (Chakraborty et al., 2020; He et al., 2016). This class of bacteria are widely found in bioelectrochemical denitrifying reactors (Pous et al., 2015b). At genus level, both reactors were clearly dominated by *Sideroxydans* (80-54%), *Denitratisoma* (4-5%) and *Achromobacter* (2-5%). *Sideroxydans lithotrophicus* ES-1 is included in the *Gallionellaceae* family and is reported as Fe(II) oxidizing chemoautotrophic bacteria. Some studies revealed its presence in autotrophic Fe(II)-oxidizing and nitrate-reducing enrichment culture (Shelobolina et al., 2012). Recently, it was reported that *Gallinionellaceae* sp. are not necessarily able to perform the complete denitrification process (He et al., 2016). The presence of other denitrifiers (e.g., *Achromobacter agilis* and *Denitratisoma oestradiolicum*) should be required for complete denitrification through cooperative sequential reactions. In addition, some studies revealed that *Sideroxydans lithotrophicus* grows when treating an arsenic-contaminated groundwater with nitrate (Chakraborty et al., 2020) suggesting that this genus is resistant to an arsenic-rich environment and may be involved in redox cycling of arsenic, too.

Betaproteobacteriales are also involved in redox cycling of arsenic. In particular, *Achromobacter* spp. has been described as autotrophic bacterial capable of arsenite oxidation using oxygen (Nguyen et al., 2017), nitrate (Su et al., 2018) or an electrode as electron acceptor (Nguyen et al., 2016b; Pous et al., 2015a). Indeed, the genetic analyses of the bioanodes revealed a high relative abundance of *Achromobacter agilis* (77-47%). Thus, this microbial community could perform three arsenite oxidation pathways that were previously discussed (Fig. 3C and D). However, as it was demonstrated that bioelectrochemical arsenite oxidation is not likely to occur (please see Section 3.2.), arsenite oxidation coupled

Table 3
Most abundant amplicon sequence variant (ASVs) at a genus level after comparison of sequences with the NCBI GenBank database.

Number ASVs	Most probable identification	Sequence Similarity (% similarity)	Relative abundance (% of sequences)			
			Reactor A		Reactor B	
			Biofilm Anode	Biofilm Cathode	Biofilm Anode	Biofilm Cathode
Betaproteobacteriales						
ASV1	(NR_152013.1) *Achromobacter agilis* strain LMG 3411	100	73.8 ± 8.5	2.2 ± 1.8	45.7 ± 9.3	4.8 ± 0.5
ASV8	(NR_152013.1) *Achromobacter agilis* strain LMG 3411	99.6	2.9 ± 04	<0.1	1.8 ± 0.3	0.2 ± 0.0
ASV2	(NR_074731.1) *Sideroxydans lithotrophicus* ES-1	96.44	<0.1	70.7 ± 2.7	2.1 ± 2.8	51.9 ± 2.9
ASV10	(NR_074731.1) *Sideroxydans lithotrophicus* ES-1	96.05	ND	2.6 ± 0.0	<0.1	1.9 ± 0.1
ASV5	(NR_043249.1) *Denitratisoma oestradiolicum* strain AcBE2-1	96.05	ND	4.3 ± 0.5	0.4 ± 0.5	4.8 ± 0.1
Rhizobiales						
ASV6	(NR_133841.1) *Rhizobium azibense* strain 23C2	99.6	1.6 ± 2.3	<0.1	8.4± 0.4	<0.1
ASV3	(NR_074219.1) *Starkeya novella* DSM 506	98.81	3.7 ± 5.2	0.4 ± 0.3	22.4 ± 11.0	0.3 ± 0.1
Actinobacteria						
ASV9	(NR_115708.1) *Rhodococcus qingshengii* strain djl-6-2	100	4.7 ± 1.7	0.3 ± 0.2	2.7 ± 0.4	0.7 ± 0.1
Bacteroidia						
ASV4	(NR_117435.1) *Ohtaekwangia koreensis* strain 3B-2	95.2	<0.1	7.5 ± 0.4	0.2 ± 0.2	7.9 ± 0.2

to denitrification is the most probable pathway (Fig. 3B). This hypothesis is further supported by the consideration that the usage of a soluble electron acceptor (e.g., nitrate) provides more catabolic energy for microbial growth and activity than transferring electron to an insoluble electron acceptor (e.g., electrode) (Korth and Harnisch, 2019).The arsenite oxidation linked to nitrate reduction could be carried out in both compartments as *Achromobacter agilis* is also present also in the biocathode (2-5 %).

3.4. Electrochemical characterization of denitrifying biocathodes by sampling single granules

The electrochemical characterisation of granular graphite electrode is challenging due to their high internal resistance. Some studies analysed the performance of a single granule fixed with a platinum wire (Borsje et al., 2016; Caizán-Juanarena et al., 2019). Nevertheless, it was recently introduced the unique approach of using the e-Clamp for analysing single granules sampled from a running bioelectrochemical bed electrode (Rodrigo Quejigo et al., 2018) Thereby single granules were sampled from the top of the cathode compartments and electrochemically analysed with the e-Clamp (see Section 2.6 and Figure S2 in Supplementary data). Chronoamperometry (CA) at -0.123 V and cyclic voltammetry (CV) were performed with granules sampled during the terminal reactor operation (days 187-194, HRT of 1.6 ± 0.1 h, n = 6). Buffer solutions without nitrate and arsenite were used in the beginning followed by the subsequent addition of nitrate (33 g N-NO_3^- m^{-1}) as well as arsenite (5 g As(III) m^{-1}) (Fig. 5).

The electrochemical characterization revealed that arsenite concentration of 5 mg L^{-1} did not inhibit the denitrifying biocathode performance (Fig. 3A). During CAs, the average specific current density was 0.07 ± 0.02 mA $g^{-1}_{graphite}$ (n = 6, Fig. 5A and B show representative results from reactor A and B, respectively) either exposed to nitrate alone or together with arsenite. CVs performed with arsenite are similar to CVs performed only with nitrate (Fig. 5C and D). The derived formal potential of the EET related to nitrate reduction was -0.02 ± 0.01 V, pH 7.75 ± 0.2. This is close to reported values for denitrifying biocathodes composed predominantly by *Betaproteobacteriales* cultivated in buffered mediums without arsenite; for example, Gregoire et al. (2014) and

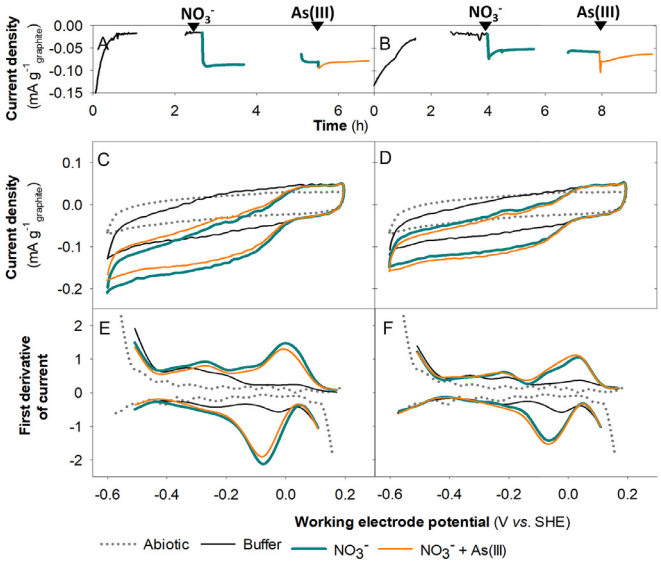

Fig. 5. Exemplary chronoamperometry (A, B), cyclic voltammetry (C, D) and corresponding first derivative (E, F). It was performed with sampled granules from reactor A (A, C and E) and with reactor B (B, D and F), and with non-inoculated graphite granules (abiotic, dashed grey line). Periods of interrupted current density indicate conduction of cyclic voltammetry (scan rate 1 mV s-1, only 3rd scans are shown). Black arrows indicate addition of nitrate and arsenite.

Pous et al. (2014) observed a formal potential of -0.03 V at pH 7 and 0.10 V at pH 8, respectively. The observation of a similar formal potentials for denitrifying biocathodes grown under different poised potentials and with different media suggested a common metabolic trait for this group of electroactive denitrifying bacteria.

4. Conclusions

The present study introduced primary microbial electrochemical technologies for the simultaneous and sustainable treatment of common groundwater pollutants. The developed system combined nitrate reduction and arsenite oxidation in a single bioelec-

trochemical reactor. Fluid dynamics was identified as an important parameter for denitrification performance and internal recirculation mitigated mass transfer limitations. Maximum nitrate reduction rate (519 g $N\text{-}NO_3^-$ m^{-3}_{NCC} d^{-1}) was achieved at HRT of 2.3 h (HRT_{cat} 1.5h) and a maximum arsenite oxidation rate of 90 g As(III) $m^{-3}_{NAC+NCC}$ d^{-1} was reached until HRT of 1.6h. Nitrate was completely converted into dinitrogen gas, reaching the effluent the standard drinking water quality in terms of nitrate and nitrite concentration (Nitrates Directive, 91/767/EU). Besides, the denitrification performance by *Sideroxydans lithotrophicus* ES-1 was not affected by arsenite (5 mg L^{-1}) in the medium. Regarding the oxidation of arsenite, several biotic and abiotic oxidation pathways played a role in the BES reactor. Nevertheless, the microbial community developed was capable of arsenic oxidation linked to denitrification in both compartments reaching high efficiencies (>95%). *Achromobacter agilis* was identified as the candidate for microbial arsenite oxidation coupled to nitrate reduction. Contrary to expectations, the biological arsenic oxidation was not sustained through the anode as a sole electron acceptor. Furthermore, abiotic experiments suggested a catalytic activity of granular graphite for arsenite oxidation through some impurities such as iron from the manufacturing process.

This research fosters the real application of electrobioremediation technology in terms of groundwater treatment with different pollutants. Thereby, MET's capability to denitrify while being unaffected by the presence of arsenite and under low electrical conductivity was proved. Moreover, the feasibility of this technology to oxidize arsenite as a pre-treatment for its removal by other methods was also demonstrated.

Declaration of Competing Interest

The authors declare that they have no known competing financial interests or personal relationships that could have appeared to influence the work reported in this paper.

Acknowledgements

This work was funded through the European Union's Horizon 2020 project ELECTRA [no. 826244]. S.P is a Serra Húnter Fellow (UdG-AG-575) and acknowledges the funding from the ICREA Acadèmia award. LEQUiA [2017-SGR-1552] and Ecoaqua [2017SGR-548] have been recognized as consolidated research groups by the Catalan Government. The authors acknowledge the Councils of Caldes de Malavella, Cervià de Ter and Navata, and Prodaisa company S.A. for their support on sampling contaminated groundwater.

Supplementary materials

Supplementary material associated with this article can be found, in the online version, at doi:10.1016/j.watres.2020.116748.

References

APHA, 2005. Standard Methods for the Examination of Water and Wastewater, 19th ed. Am. Public Heal. Assoc. Washingt. DC, USA.

Bachate, S.P., Khapare, R.M., Kodam, K.M., 2012. Oxidation of arsenite by two β-proteobacteria isolated from soil. Appl. Microbiol. Biotechnol. doi:10.1007/s00253-011-3606-7.

Balch, W.E., Fox, G.E., Magrum, L.J., Woese, C.R., Wolfe, R.S., 1979. Methanogens: reevaluation of a unique biological group. Microbiol. Rev. 43 260 LP – 296.

Banerjee, K., Amy, G.L., Prevost, M., Nour, S., Jekel, M., Gallagher, P.M., Blumenschein, C.D., 2008. Kinetic and thermodynamic aspects of adsorption of arsenic onto granular ferric hydroxide (GFH). Water Res. doi:10.1016/j.watres.2008.04.019.

Bissen, M., Frimmel, F.H., 2003. Arsenic - a review. Part II: oxidation of arsenic and its removal in water treatment. Acta Hydrochim. Hydrobiol. 31, 97–107. doi:10.1002/aheh.200300485.

Borho, M., Wilderer, P., 1996. Optimized removal of arsenate(III) by adaptation of oxidation and precipitation processes to the filtration step. Water Science and Technology doi:10.1016/S0273-1223(96)00783-4.

Borsje, C., Liu, D., Sleutels, T.H.J.A., Buisman, C.J.N., ter Heijne, A., 2016. Performance of single carbon granules as perspective for larger scale capacitive bioanodes. J. Power Sources doi:10.1016/j.jpowsour.2016.06.092.

Caizán-Juanarena, L., Servin-Balderas, I., Chen, X., Buisman, C.J.N., ter Heijne, A., 2019. Electrochemical and microbiological characterization of single carbon granules in a multi-anode microbial fuel cell. J. Power Sources doi:10.1016/j.jpowsour.2019.04.042.

Callahan, B.J., McMurdie, P.J., Rosen, M.J., Han, A.W., Johnson, A.J.A., Holmes, S.P., 2016. DADA2: high-resolution sample inference from Illumina amplicon data. Nat. Methods 13, 581–583. doi:10.1038/nmeth.3869.

Chakraborty, A., DasGupta, C.K., Bhadury, P., 2020. Diversity of Betaproteobacteria revealed by novel primers suggests their role in arsenic cycling. Heliyon. 10.1016/j.heliyon.2019.e03089

Chen, W., Parette, R., Zou, J., Cannon, F.S., Dempsey, B.A., 2007. Arsenic removal by iron-modified activated carbon. Water Res. doi:10.1016/j.watres.2007.01.052.

Clauwaert, P., Desloover, J., Shea, C., Nerenberg, R., Boon, N., Verstraete, W., 2009. Enhanced nitrogen removal in bio-electrochemical systems by pH control. Biotechnol. Lett. doi:10.1007/s10529-009-0048-8.

Clauwaert, P., Rabaey, K., Aelterman, P., De Schamphelaire, L., Pham, T.H., Boeckx, P., Boon, N., Verstraete, W., 2007. Biological denitrification in microbial fuel cells. Environ. Sci. Technol. doi:10.1021/es062580r.

Crognale, S., Amalfitano, S., Casentini, B., Fazi, S., Petruccioli, M., Rossetti, S., 2017. Arsenic-related microorganisms in groundwater: a review on distribution, metabolic activities and potential use in arsenic removal processes. Rev. Environ. Sci. Biotechnol. 16, 647–665. doi:10.1007/s11157-017-9448-8.

European Commission, 2008. Groundwater Protection in Europe: the New Groundwater Directive - Consolidating the EU Regulatory Framework. Office for Official Publications of the European Communities doi:10.2779/84304.

Fourmond, V., Hoke, K., Heering, H.A., Baffert, C., Leroux, F., Bertrand, P., Léger, C., 2009. SOAS: a free program to analyze electrochemical data and other one-dimensional signals. Bioelectrochemistry doi:10.1016/j.bioelechem.2009.02.010.

Glass, C., Silverstein, J., 1998. Denitrification kinetics of high nitrate concentration water: pH effect on inhibition and nitrite accumulation. Water Res. doi:10.1016/S0043-1354(97)00260-1.

Gregoire, K.P., Glaven, S.M., Hervey, J., Lin, B., Tender, L.M., 2014. Enrichment of a high-current density denitrifying microbial biocathode. J. Electrochem. Soc. 161, H3049–H3057. doi:10.1149/2.0101413jes.

Gregory, K.B., Bond, D.R., Lovley, D.R., 2004. Graphite electrodes as electron donors for anaerobic respiration. Environ. Microbiol. doi:10.1111/j.1462-2920.2004.00593.x.

He, S., Tominski, C., Kappler, A., Behrens, S., Roden, E.E., 2016. Metagenomic analyses of the autotrophic Fe(II)-oxidizing, nitrate-reducing enrichment culture KS. Appl. Environ. Microbiol. 82. doi:10.1128/AEM.03493-15.

Hosono, T., Nakano, T., Shimizu, Y., Onodera, S.I., Taniguchi, M., 2011. Hydrogeological constraint on nitrate and arsenic contamination in Asian metropolitan groundwater. Hydrol. Process. doi:10.1002/hyp.8015.

Jang, Y.-C., Somanna, Y., Kim, H., 2016. Source, distribution, toxicity and remediation of arsenic in the environment – a review. Int. J. Appl. Environ. Sci. ISSN.

Ji, Y., Wang, L., Jiang, M., Lu, J., Ferronato, C., Chovelon, J.M., 2017. The role of nitrite in sulfate radical-based degradation of phenolic compounds: an unexpected nitration process relevant to groundwater remediation by in-situ chemical oxidation (ISCO). Water Res. doi:10.1016/j.watres.2017.06.081.

Korth, B., Harnisch, F., 2019. Spotlight on the energy harvest of electroactive microorganisms: the impact of the applied anode potential. Front. Microbiol. doi:10.3389/fmicb.2019.01352.

Kozich, J.J., Westcott, S.L., Baxter, N.T., Highlander, S.K., Schloss, P.D., 2013. Development of a dual-index sequencing strategy and curation pipeline for analyzing amplicon sequence data on the miseq illumina sequencing platform. Appl. Environ. Microbiol. doi:10.1128/AEM.01043-13.

Lai, A., Aulenta, F., Mingazzini, M., Palumbo, M.T., Papini, M.P., Verdini, R., Majone, M., 2017. Bioelectrochemical approach for reductive and oxidative dechlorination of chlorinated aliphatic hydrocarbons (CAHs). Chemosphere doi:10.1016/j.chemosphere.2016.11.072.

Lai, A., Verdini, R., Aulenta, F., Majone, M., 2015. Influence of nitrate and sulfate reduction in the bioelectrochemically assisted dechlorination of cis-DCE. Chemosphere doi:10.1016/j.chemosphere.2014.12.023.

Li, Yunlong, Zhang, B., Cheng, M., Li, Yalong, Hao, L., Guo, H., 2016. Spontaneous arsenic (III) oxidation with bioelectricity generation in single-chamber microbial fuel cells. J. Hazard. Mater. doi:10.1016/j.jhazmat.2015.12.003.

Logan, B.E., Rossi, R., Ragab, A., Saikaly, P.E., 2019. Electroactive microorganisms in bioelectrochemical systems. Nat. Rev. Microbiol. doi:10.1038/s41579-019-0173-x.

McMurdie, P.J., Holmes, S., 2013. Phyloseq: an R package for reproducible interactive analysis and graphics of microbiome census data. PLoS One 8, e61217. doi:10.1371/journal.pone.0061217.

Molognoni, D., Devecseri, M., Cecconet, D., Capodaglio, A.G., 2017. Cathodic groundwater denitrification with a bioelectrochemical system. J. Water Process Eng. 19, 67–73. doi:10.1016/j.jwpe.2017.07.013.

Nguyen, V.K., Park, Y., Yang, H., Yu, J., Lee, T., 2016a. Effect of the cathode potential and sulfate ions on nitrate reduction in a microbial electrochemical denitrification system. J. Ind. Microbiol. Biotechnol. doi:10.1007/s10295-016-1762-6.

Nguyen, V.K., Park, Y., Yu, J., Lee, T., 2016b. Simultaneous arsenite oxidation and nitrate reduction at the electrodes of bioelectrochemical systems. Environ. Sci. Pollut. Res. 23, 19978–19988. doi:10.1007/s11356-016-7225-9.

Nguyen, V.K., Tran, H.T., Park, Y., Yu, J., Lee, T., 2017. Microbial arsenite oxidation with oxygen, nitrate, or an electrode as the sole electron acceptor. J. Ind. Microbiol. Biotechnol. 44, 857–868. doi:10.1007/s10295-017-1910-7.

Piqué, À., Grandia, F., Canals, À., 2010. Processes releasing arsenic to groundwater in the Caldes de Malavella geothermal area. NE Spain. Water Res. doi:10.1016/j.watres.2010.07.012.

Pous, N., Balaguer, M.D., Colprim, J., Puig, S., 2018. Opportunities for groundwater microbial electro-remediation. Microb. Biotechnol. 11, 119–135. doi:10.1111/1751-7915.12866.

Pous, N., Casentini, B., Rossetti, S., Fazi, S., Puig, S., Aulenta, F., 2015a. Anaerobic arsenite oxidation with an electrode serving as the sole electron acceptor: A novel approach to the bioremediation of arsenic-polluted groundwater. J. Hazard. Mater. 283, 617–622. doi:10.1016/j.jhazmat.2014.10.014.

Pous, N., Koch, C., Colprim, J., Puig, S., Harnisch, F., 2014. Extracellular electron transfer of biocathodes: revealing the potentials for nitrate and nitrite reduction of denitrifying microbiomes dominated by Thiobacillus sp. Electrochem. Commun. 49, 93–97. doi:10.1016/j.elecom.2014.10.011.

Pous, N., Puig, S., Balaguer, M.D., Colprim, J., 2017. Effect of hydraulic retention time and substrate availability in denitrifying bioelectrochemical systems. Environ. Sci. Water Res. Technol. 3, 922–929. doi:10.1039/c7ew00145b.

Pous, N., Puig, S., Coma, M., Balaguer, M.D., Colprim, J., 2013. Bioremediation of nitrate-polluted groundwater in a microbial fuel cell. J. Chem. Technol. Biotechnol. doi:10.1002/jctb.4020.

Pous, N., Puig, S., Dolors Balaguer, M., Colprim, J., 2015b. Cathode potential and anode electron donor evaluation for a suitable treatment of nitrate-contaminated groundwater in bioelectrochemical systems. Chem. Eng. J. 263, 151–159. doi:10.1016/j.cej.2014.11.002.

Puig, S., Coma, M., Desloover, J., Boon, N., Colprim, J., Balaguer, M.D., 2012. Autotrophic denitrification in microbial fuel cells treating low ionic strength waters. Environ. Sci. Technol. doi:10.1021/es2030609.

Rodrigo Quejigo, J., Rosa, L.F.M., Harnisch, F., 2018. Electrochemical characterization of bed electrodes using voltammetry of single granules. Electrochem. Commun. 90, 78–82. doi:10.1016/j.elecom.2018.04.009.

Shelobolina, E., Xu, H., Konishi, H., Kukkadapu, R., Wu, T., Blöthe, M., Roden, E., 2012. Microbial lithotrophic oxidation of structural Fe(II) in biotite. Appl. Environ. Microbiol. 78. doi:10.1128/AEM.01034-12.

Su, J., Liang, D., Lian, T., 2018. Comparison of denitrification performance by bacterium Achromobacter sp. A14 under different electron donor conditions. Chem. Eng. J. 333, 320–326. doi:10.1016/j.cej.2017.09.129.

Sun, W., Sierra-Alvarez, R., Hsu, I., Rowlette, P., Field, J.A., 2009. Anoxic oxidation of arsenite linked to chemolithotrophic denitrification in continuous bioreactors. Biotechnol. Bioeng. doi:10.1002/bit.22611.

Sun, W., Sierra, R., Field, J.A., 2008. Anoxic oxidation of arsenite linked to denitrification in sludges and sediments. Water Res. doi:10.1016/j.watres.2008.08.004.

Twomey, K.M., Stillwell, A.S., Webber, M.E., 2010. The unintended energy impacts of increased nitrate contamination from biofuels production. J. Environ. Monit. doi:10.1039/b913137j.

Van Halem, D., Bakker, S.A., Amy, G.L., Van Dijk, J.C., 2009. Arsenic in drinking water: a worldwide water quality concern for water supply companies. Drink. Water Eng. Sci. 2, 29–34. doi:10.5194/dwes-2-29-2009.

Ventura-Houle, R., Font, X., Heyer, L., 2018. Groundwater arsenic contamination and their variations on episode of drought: Ter River delta in Catalonia, Spain. Appl. Water Sci. doi:10.1007/s13201-018-0772-0.

Vilajeliu-Pons, A., Bañeras, L., Puig, S., Molognoni, D., Vilà-Rovira, A., Amo, E.H.Del, Balaguer, M.D., Colprim, J., 2016. External resistances applied to MFC affect core microbiome and swine manure treatment efficiencies. PLoS One doi:10.1371/journal.pone.0164044.

Virdis, B., Rabaey, K., Yuan, Z., Keller, J., 2008. Microbial fuel cells for simultaneous carbon and nitrogen removal. Water Res. 42, 3013–3024. doi:10.1016/j.watres.2008.03.017.

Wang, H., Zhang, S., Wang, J., Song, Q., Zhang, W., He, Q., Song, J., Ma, F., 2018. Comparison of performance and microbial communities in a bioelectrochemical system for simultaneous denitrification and chromium removal: effects of pH. Process Biochem. doi:10.1016/j.procbio.2018.08.007.

Li, Hongli, Li, Haisong Wang, J., Wan, J., Wu, Z., Dagot, C., Wang, Y., 2017. Flexible biological arsenite oxidation utilizing NOx and O2 as alternative electron acceptors. Chemosphere doi:10.1016/j.chemosphere.2017.03.044.

Wang, S., Zhao, X., 2009. On the potential of biological treatment for arsenic contaminated soils and groundwater. J. Environ. Manage. doi:10.1016/j.jenvman.2009.02.001.

WHO, 2017. Guidelines for Drinking-Water Quality: Fourth Edition Incorporating the First Addendum. World Health Organization doi:10.5942/jawwa.2017.109.0087.

Zhang, S., Mao, G., Crittenden, J., Liu, X., Du, H., 2017. Groundwater remediation from the past to the future: a bibliometric analysis. Water Res. doi:10.1016/j.watres.2017.01.029.